


Article

Experimental and Analytical Studies of Reciprocating Flow Heat Transfer in a Reciprocating Loop Device for Electronics Cooling

Mohammad Didarul Alam ^{*}, Majid Almas, Soheil Soleimanikutanaei and Yiding Cao

Department of Mechanical and Materials Engineering, Florida International University (FIU), Miami, FL 33174, USA; majidaaia@gmail.com (M.A.); ssole016@fiu.edu (S.S.); caoy@fiu.edu (Y.C.)

^{*} Correspondence: malam052@fiu.edu

Abstract: The thermal management of electronics is essential, since their lifetime and reliability are highly dependent on their operating temperature and temperature uniformity. Regarding that, Reciprocating-Mechanism Driven Heat Loop (RMDHL) technology has been invented and shows potentiality to become an effective high heat flux cooling system. In this paper, the performance of a reciprocating cooling loop, in terms of heat transfer and temperature distribution, is studied experimentally and analytically. The experimental results showed that, as the reciprocating flow amplitude increases, the loop surface temperature decreases, and the temperature uniformity along the loop improves. However, in contrast to the amplitude effect, a higher frequency may not necessarily improve the temperature uniformity, although the condenser section temperature may be lower. Further, adiabatic section temperature appears to be insensitive to the reciprocating frequency. The experimental results were then summarized in a semi-empirical correlation that demonstrates a useful design tool for the thermal engineer community. Additionally, the analytical results provide critical design requirements that should be considered during Reciprocating-Mechanism Driven Heat Loop (RMDHL) system design.

Keywords: electronics cooling; oscillatory flow; experimental study; analytical modeling



Citation: Alam, M.D.; Almas, M.; Soleimanikutanaei, S.; Cao, Y. Experimental and Analytical Studies of Reciprocating Flow Heat Transfer in a Reciprocating Loop Device for Electronics Cooling. *Fluids* **2022**, *7*, 132. <https://doi.org/10.3390/fluids7040132>

Academic Editors: Mehrdad Massoudi and Pouyan Talebizadeh Sardari

Received: 21 February 2022

Accepted: 4 April 2022

Published: 8 April 2022

Publisher's Note: MDPI stays neutral with regard to jurisdictional claims in published maps and institutional affiliations.



Copyright: © 2022 by the authors. Licensee MDPI, Basel, Switzerland. This article is an open access article distributed under the terms and conditions of the Creative Commons Attribution (CC BY) license (<https://creativecommons.org/licenses/by/4.0/>).

1. Introduction

Present-day sophisticated electronics have created significant challenges to their thermal management due to their robust performance improvement, size compactness, and working conditions. During operation, the associated heat flux increases exponentially in modern-day electronics. For example, a heat flux level of 120–150 W/cm² has already been reached in some electronics applications and the trend is perpetually rocketing [1], while, on the contrary, traditional thermal management systems are continuously facing difficulties to meet this growing challenge and, in some circumstances, they have proven inadequate. It should be noted that the electronic component's lifetime and reliability are highly vulnerable to their operating temperature, as well as temperature uniformity. As a result, highly efficient thermal management systems are in high demand to meet this growing challenge.

Several emerging technologies show the potential to become high heat flux electronics cooling systems: innovation of several types of heat sinks, thermoelectric coolers, forced air systems and fans, nano-fluids, microchannels, nanoporous membrane tubes, impingement and spray cooling, etc. [2–8]. Narcy et al. [9] proposed a novel type of two-phase heat spreader for electronics cooling applications, which is based on a flat confined thermosiphon system. The study primarily investigated its thermal performance and flow visualization. Based on the findings, it appears that confined fluid inside the heat spreader increases the degree of freedom of the heat source's location and induces a confined boiling phenomenon. Furthermore, robust coupling between boiling mechanisms and condensation was observed

and the system's sensitivity to inclination angle is relatively low. Likewise, a miniature vapor compression refrigeration system was deployed for electronics cooling, where the evaporator consisted of a micro-channel heat sink [10]. The refrigeration system's purpose was to control and maintain the heat source surface temperature within a suitable range. The study concluded that the surface temperature of the heater could decrease if the compressor speed increases. However, it will also decrease the coefficient of performance (COP). A detail of the current state of the art, involving traditional and emerging electronics cooling methods, and related coolants, can be found in work conducted by Murshed and Castro [11].

Another potential trend over the past few decades is the application of oscillatory flow in electronics thermal management systems that facilitates enhancing heat transfer capability compared with unidirectional flow. For instance, Mackley and Stonestreet [12] showed experimentally that the oscillatory flow has a significant heat transfer enhancement capability in the periodically baffled tube compared to unidirectional flow. Within the study, different important heat transfer parameters were studied: Prandtl (Pr) numbers, penetration length, Womersley, etc. Moreover, a correlation for Nusselt Number and dynamic pressure of the flow was established based on the experimental results. The Nusselt number, as well as the instantaneous and time-average bulk temperature, showed that when the Prandtl number and penetration length increased, the overall convective heat transfer increased. Similarly, heat transfer phenomena for oscillatory flow were examined in a circular tube by Bouvier et al. [13]. The heat conduction inverse method, and the local heat transfer, was characterized in their study. To gauge the onset of turbulence in the oscillatory flow, Zhao and Cheng [14] presented a correlation in terms of kinetic Reynolds number and amplitude of the flow. The effect of frictional loss and transition to turbulence were also investigated for their oscillatory airflow. In literature, computational fluid dynamics widespread use has also been observed to study the flow and heat transfer phenomena [15,16]. The application of a flow pulsation waveform in a mesochannel for heat transfer was inspected by McEvoy et al. [17] and a recent review regarding mechanically driven oscillatory flow can be found in the literature [18].

Along with other promising technologies, Reciprocating-Mechanism Driven Heat Loop (RMDHL) is an excellent addition to the current state of the art in high heat flux electronics cooling systems. The RMDHL [19–21] is a liquid-based cooling device that works by changing the flow direction between the heat sink and the heat source on a continual basis within the device. Compared to typical Dynamic Pump-Driven Heat Loops (DPDHL), the RMDHL provides a superior cooling performance. Several studies have already shown its advantage over conventional systems. For instance, Cao and Gao [22] introduced a solenoid-driven Reciprocating-Mechanism to produce necessary oscillatory flow. It was intended for two-phase cooling applications, which can handle a high heat flux of up to 300 W/cm^2 . In addition to the RMDHL superior heat transfer performance, the flow mechanism could also suppress the cavitation problem that might occur within conventional pumps. The similar superior performance of the RMDHL over the DPDHL system, in terms of surface temperature uniformity and heat transfer, was also observed in the investigation of Soleimanikutanaei et al. [23]. The research developed a numerical model to study the reciprocating motion flow for the desired frequency. For a given mass flow rate, the average surface temperature in the RMDHL was substantially less than the DPDHL. Popoola et al. [24] analyzed the heat transfer phenomena for an RMDHL loop, both experimentally and numerically. Their reciprocating flow was driven via piston-cylinder-mechanism and the constant heat flux was applied to the evaporator. Along with the investigation of heat transfer phenomena, they established a Nusselt number correlation for the loop cycle. The accuracy of different turbulence models during the analysis of the RMDHL loop performance was also investigated and summarized [25]. The research findings show that for the calculation of the average cold plate temperature, the standard $k-\epsilon$ Model is more accurate, whereas, for the cold plate surface temperature, the RNG $k-\epsilon$ Model shows more accuracy. In similar fashion, Sert and Beskok [26] numerically examined

reciprocating flow in a two-dimensional channel under forced convection conditions. They determined the heat transfer rate in terms of the penetration length, Womersley (α) number, Prandtl (Pr) number, bulk temperature distributions, and the instantaneous and time-averaged surface temperature. Furthermore, they developed a comparison between the reciprocating flow and unidirectional flows.

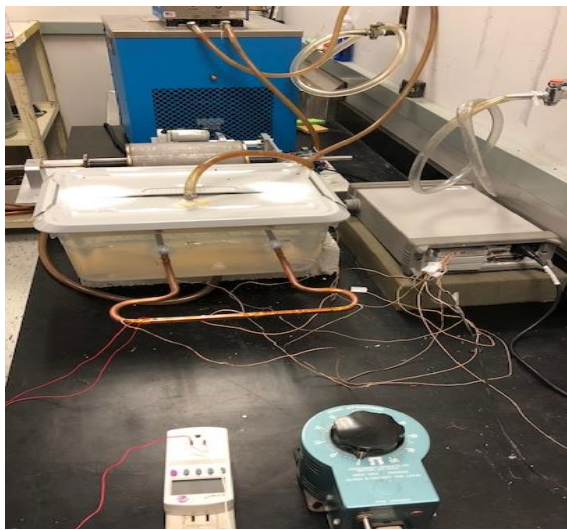
The present study is another advancement on RMDHL and maintains significance, as well as novelty, in several ways. Firstly, the above-cited studies regarding the RMDHL loop are mostly concentrated on reciprocating flow in a duct, not at the system level, whereas the present design is implemented in the system-level application and is essential for its successful demonstration. Secondly, previous studies focused more on thermal performance. In contrast, the present study investigates in more detail the effect of different important design parameters that should be considered during its design stages. Thirdly, the current loop has been tested for a wide range of heat transfer distances and rates, as opposed to previous studies, with limited heat transfer distances and rates. Finally, analytical models related to the reciprocating loop design criteria and performance have been developed, and the model's results have also been compared with the available experimental results. Therefore, combining all these together justifies the significance and novelty of the current work.

Here, Section 2 presents the experimental setup. The results and discussion are presented in Section 3, followed by effective heat transfer conductance and correlation in Section 3.1. Section 4 presents the critical displacement volume of the RMDHL, followed by the conclusion in Section 5.

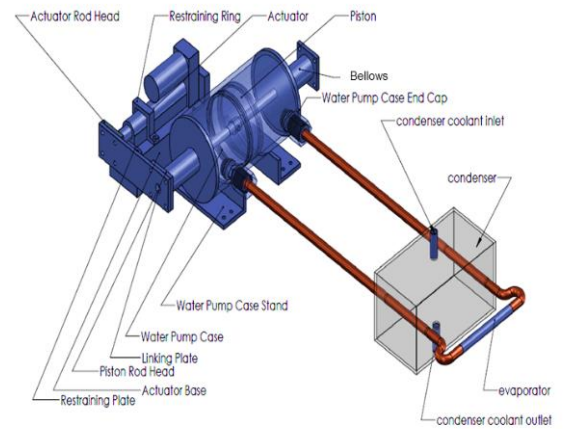
2. Experimental Setup

A bellows-type reciprocating heat transfer device was constructed on the basis of Cao et al. [27]. The device is designed to handle high heat transfer rates with a single-phase flow. The setup, CAD drawing of the test rig, the schematic of the cooling loop, and the locations of the thermocouples (102 to 107) are shown in Figure 1a–c.

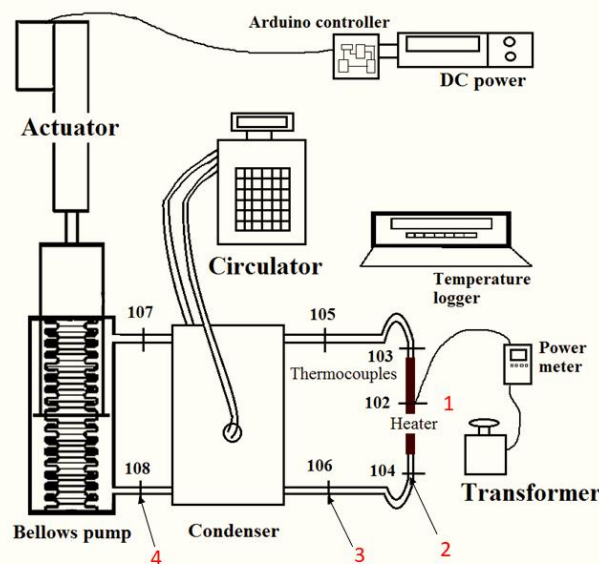
The reciprocating driver includes an actuator-driven piston in conjunction with two bellows for sealing purposes. The inner diameter of the bellows is 2.70 cm with 50 turns. They are attached to the driver mechanism at each end of the chamber to facilitate the reciprocating motion of the piston while maintaining the chamber in a hermetic condition. An Arduino controls the driving mechanism and the Progressive Automations Linear Actuator, while a force of 150 lbs drives the piston. A circuit board has been used to regulate the actuator DC power supply. The setup uses a flexible heater KH-108 Omega lux flexible heater, 100 W (manufactured by Omega Engineering, Stamford, CT, USA), and a Polystat thermal bath with a temperature range from -20 °C to 150 °C that maintains a constant temperature for the cooling water. The Staco power regulator in conjunction with a P4400 Wattmeter (manufactured by Prodigit Electronics, New Taipei City, Taiwan) connected to the flexible heater was employed to generate and measure the heat input in the evaporator section. An HP 34970A Data Acquisition unit (manufactured by Bell Electronics NW, Inc., Renton, WA, USA) records the temperatures for each given point. Appendix A summarized each component's details for the present experiment. Copper tubing has been selected for heat loop having an outer diameter of 14.32 mm and a wall thickness of 0.889 mm. Low thermal conductivity woven fiberglass tape was used for the insulation purpose to prevent heat loss from the experimental setup.



(a)



(b)



(c)

Figure 1. (a) Photo of the test rig assembly (b) schematic representation of the test rig assembly, and (c) location of the thermocouples with assigned positions 1, 2, 3, 4.

When the thermal bath reached the required cooling temperature, the operation of the linear actuator was initiated while the heat input to the evaporator heater gradually ramped to a test level. After the heat loop reached a steady-state condition, the temperatures were recorded on the PC using the Agilent BenchLink Data Logger software (Version 4.3, Agilent technologies, Santa Clara, CA, USA). It should be noted that water has been used to transport heat within the pipe as it has widespread applications for cooling purpose [28,29]. However, the measured temperature in the thermocouple represents the surface temperature of the pipe, not the water inside. The reciprocating frequency, driver stroke or amplitude of the reciprocating flow inside the cooling loop, heat transfer rate, power input to the actuator, and the inlet cooling temperature of the condenser water were also recorded.

3. Results and Discussion

To investigate the effect of different operational parameters on RMDHL performance, the average temperature values in the condenser, adiabatic, and evaporator sections were calculated by using thermocouples:

$$T4 \text{ (condenser)} = 0.5 \times (T107 + T108)$$

$$T3 \text{ (adiabatic section)} = 0.5 \times (T105 + T106)$$

$$T2 \text{ (evaporator section)} = 0.5 \times (T103 + T104)$$

$$T1 = T102$$

where T102 to T108 are the temperatures recorded by the thermocouples located in the test rig, according to Figure 1c. In this experiment, the experimental uncertainty sources are only the instruments. The scanning thermocouple thermometer has an accuracy of $\pm 0.1\%$ of reading $\pm 0.4 \text{ }^\circ\text{C}$ and the power meter has an accuracy of $\pm (1\% \text{ reading} + 5 \text{ digits})$. Therefore, the maximum uncertainty for the temperature and heating power measurement would be 1.0% and 2%, respectively.

It should be noted that the experiment was conducted for a wide range of variations for each input parameter, so that it can determine the significance of each parameter's effect. During the experiment, the input power in the evaporator section varied from 20 W to 90 W, the amplitude varied from 2 cm to 3.9 cm, and the reciprocation amplitude indicates the displacement of the piston from its initial position in centimeters. Similarly, the reciprocating frequency varied from 13 s/cycle to 20 s/cycle and the cooling water temperature varied from 15 $^\circ\text{C}$ to 30 $^\circ\text{C}$. However, for brevity, the important finding of the study has been plotted and presented within a couple of cases. For instance, the effect of the reciprocating amplitude on the temperature distribution in the RMDHL is shown in Figure 2, under the conditions of input power = 20 W and 60 W, reciprocating frequency in terms of a second per reciprocating cycle = 20 s/cycle, and cooling-water inlet temperature = 20 $^\circ\text{C}$. Figure 2a,b shows that as the amplitude of the reciprocating flow increases, the loop surface temperature decreases, and the temperature uniformity along the loop improves. Notably, the loop surface temperature improvement is more obvious for amplitude 2.0 to 2.5 than for amplitude 3.9 cm at a higher power input. It is believed that the ideal cooling condition for the loop performance would exist when the heated fluid in the hot region could fully move to the cold region. If the reciprocating amplitude is less than the minimum requirement, the heated water could not effectively reach the loop cold region. As a result, the heat transfer rate would decrease, and the temperature gradient would increase significantly.

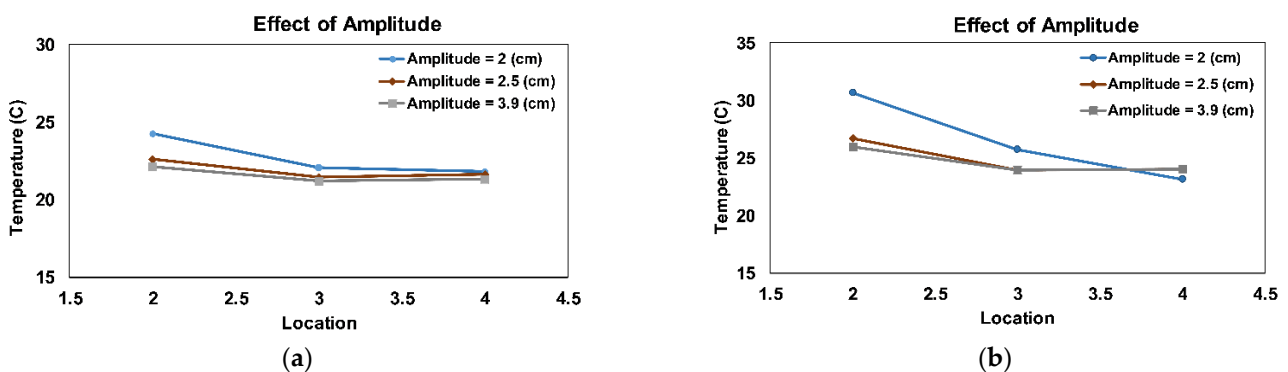


Figure 2. Effect of the amplitude on the surface temperature of the RMDHL, (a) input power 20 W (b) input power 60 W.

Similarly, the effect of reciprocating frequency in terms of time per cycle on the temperature distribution along the cooling loop is shown in Figure 3, when input powers are 20 W and 60 W, amplitude is 3.9 cm, and cooling water temperature is 20 $^\circ\text{C}$. As can be seen from the figure, both a higher frequency of 13 s/cycle and a lower frequency of 20 s/cycle result in a higher temperature gradient along the loop, while a moderate frequency of 16 s/cycle produces a much more uniform temperature. In contrast to the

effect of the amplitude, a higher frequency may not necessarily improve the temperature uniformity, although the temperature in the evaporator section may be lower. Furthermore, the temperature in the adiabatic section appears to be insensitive to the reciprocating frequency. Therefore, it is noticeable that the effect of amplitude is much more significant compared with the reciprocating frequency on the RMDHL performance.

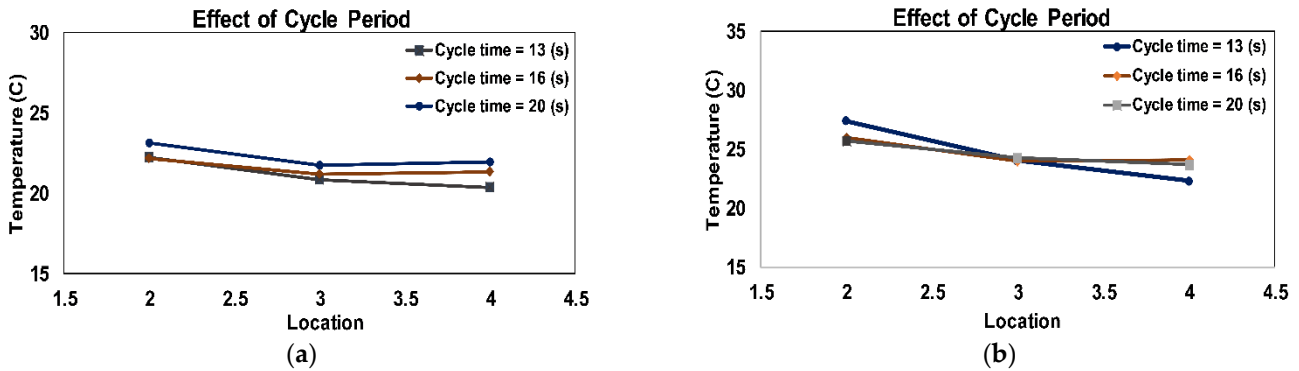


Figure 3. Effect of cycle period on the surface temperature of RMDHL, (a) input power 20 W (b) input power 60 W.

Figure 4 illustrates the effect of the cooling water inlet temperature on the surface temperature of the RMDHL, for a temperature range of 15 °C to 30 °C. The input powers are 20 W and 60 W, and the frequency and amplitude, respectively, are 16 s/cycle and 2.5 cm. Like many other heat transfer devices, the cooling water temperature controls the temperature level of the loop, and a lower cooling water temperature produces a lower loop temperature level.

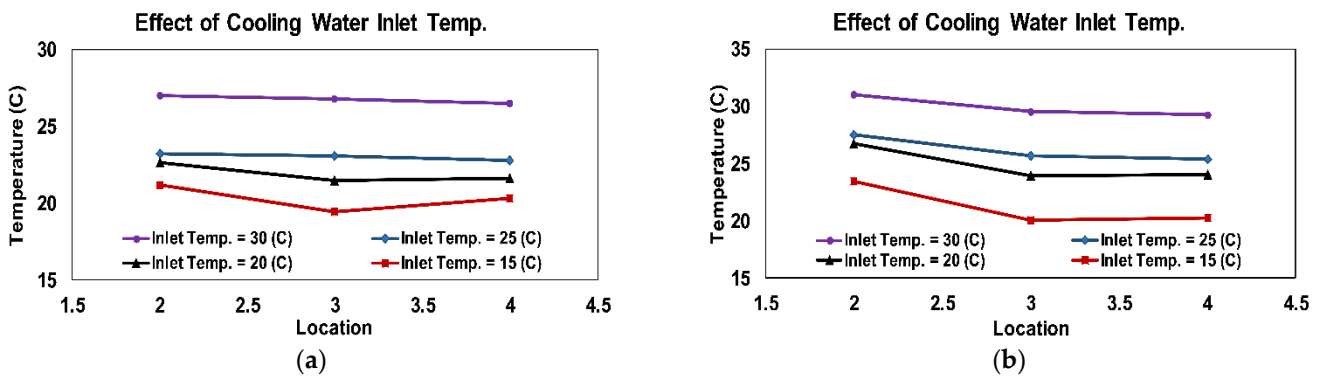


Figure 4. Effect of cooling water inlet temperature on the surface temperature of RMDHL, (a) input power 20 W, (b) input power 60 W.

The effect of the input power of the flexible heater on the temperature distribution along the RMDHL is shown in Figure 5, under the conditions of constant cooling water temperature = 20 °C, cycle frequency = 16 s/cycle, and amplitude = 2.5 cm and 3.9 cm. As expected, a higher heat input would increase both the temperature level and temperature gradient along the loop, where the temperature gradient is primarily caused by heat transfer in the evaporator section. It is obvious from Figure 5 that rising amplitude improves the temperature gradient along the loop for each power input. The temperature gradient from the adiabatic section to the condenser section is almost zero, as evidenced by the almost identical readings of T4 and T3, due to the effective water cooling in the condenser section.

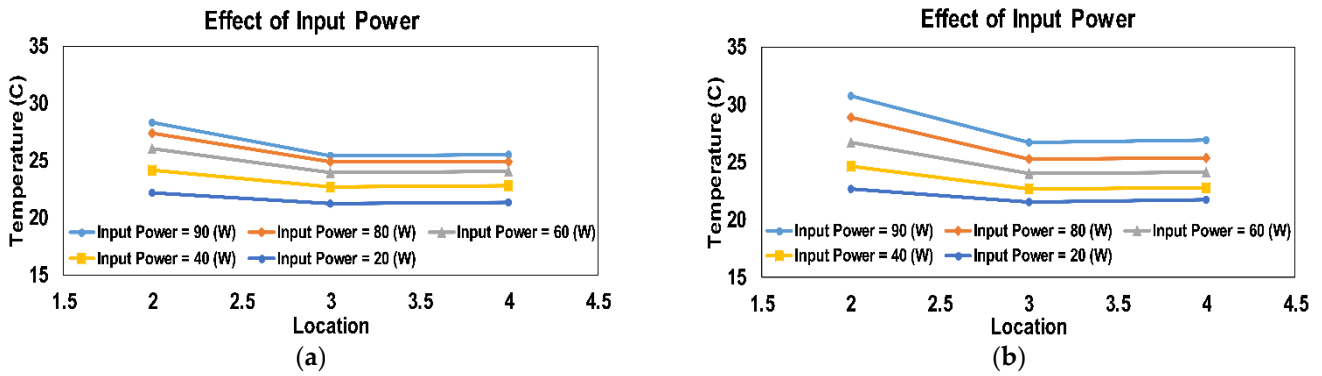


Figure 5. Effect of input power on the surface temperature of the RMDHL. (a) input amplitude 2.5 cm (b) input amplitude 3.9 cm.

3.1. Effective Heat Transfer Conductance and Correlation

The system’s effective heat transfer conductance—an important design parameter—has also been investigated. It is widely used to gauge the performance of heat pipes and can be evaluated according to the following relationship:

$$k_{eff} = \frac{QL}{A\Delta T} \tag{1}$$

where Q represents the heat input, L represents the effective distance between evaporative and condensation sections, ΔT is the temperature difference between the evaporative section and condensation section, and A represents the loop tube cross-section area, which is calculated based on the outer diameter. Figure 6 represents a schematic diagram of the present experimental setup with associated necessary dimensions.

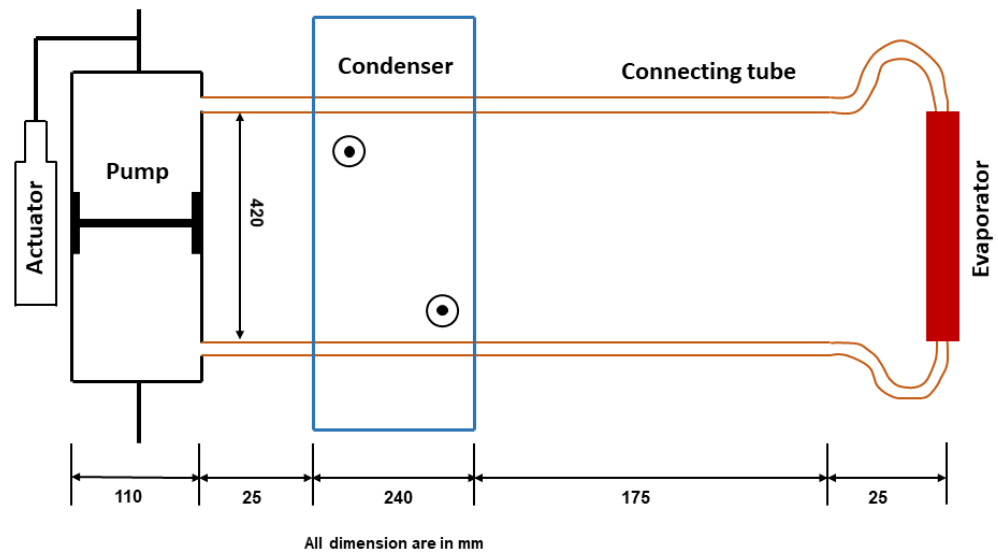


Figure 6. Experimental setup.

A sample calculation for 40 W heat input in the evaporative section is shown as follows:

$$k_{eff} = \frac{(40)(0.440)}{(1.417 \times 10^{-4})(1.5)} = 82,804.9 \text{ W/m}\cdot\text{K} \tag{2}$$

If the copper thermal conductivity is considered to be 400 W/(m·K) the dimensionless effective heat transfer conductance would be for the 40 W heat input.

$$\frac{k_{eff}}{k} = 207.01 \tag{3}$$

It seems that the RMDHL in this study is a very effective heat transfer device—the thermal conductance of RMDHL is more than 200 times higher than the copper thermal conductance at 40 W power input. For general application, a correlation for dimensionless effective heat transfer conductance has been established, in terms of flow kinematic Reynolds number $Re_\omega = \omega D^2/\nu$ and non-dimensional amplitude $A_0 = (X/D)$. Both the dimensionless parameters are specified by Cooper and Yang [30], herein the kinematic Reynolds number (also known as the Womersley number (W_0)) is calculated using the oscillation or reciprocating frequency (ω).

The Re_ω is essentially a dimensionless reciprocating frequency of the reciprocating driver, and A_0 is a dimensionless reciprocating amplitude of the driver. The reciprocating frequency ω and reciprocating amplitude X would determine the operational condition of the reciprocating driver, which, in turn, determines the performance of the reciprocating-flow loop. Since the effective heat transfer conductance k_{eff} is a major performance gauge of a reciprocating loop device, it is naturally a function of Re and A_0 , in terms of dimensionless variables. Therefore, with the help of regression analysis, the following dimensionless effective heat transfer conductance correlation has been established for the present RMDHL system:

$$\frac{k_{eff}}{k} = 413.23 Re_\omega^{-0.4840} A_0^{0.535}, \quad 14 < Re_\omega < 30 \text{ and } 2 < A_0 < 6 \quad (4)$$

Additionally, the present correlation accuracy is assessed and illustrated in Figure 7, comparing this with the experimental data. It should be noted that a reference conductivity Copper (k), the value of 400 W/m·K, has been adopted in the dimensionless effective heat conductance calculation. Most of the experimental data fall within or around +20% and −20% of the correlation predictions; an estimated error of about 20% for the current correlation.

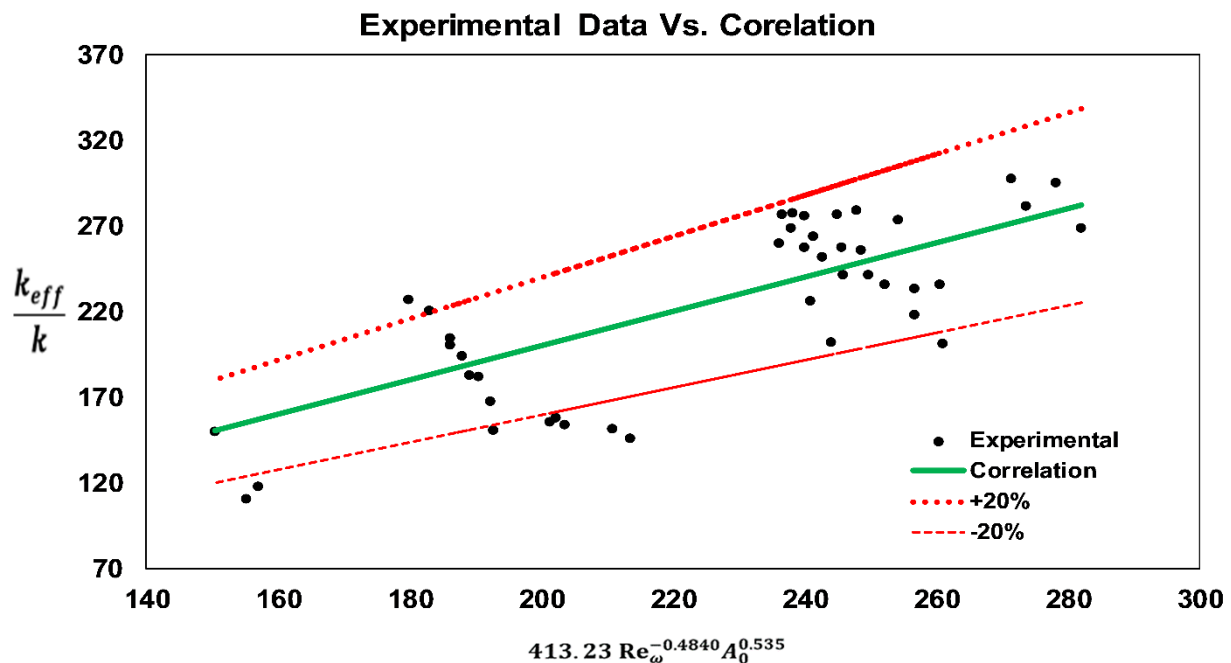


Figure 7. Comparison between the correlation and experiment data.

4. Critical Displacement Volume of the RMDHL

For successful deployment of the RMDHL in thermal management applications, the driver should work in such a way that the condenser section liquid must reach the evaporator section. As a result, a sufficiently large working fluid displacement volume (driven by the piston) is critical to ensure the adequate liquid supply between the condenser and evaporator section (cold plate) of the cooling loop. However, a larger displacement

volume demands a larger size of the liquid reservoir, subsequently, a larger cooling system. Therefore, a tradeoff must be made, not only to ensure a sufficient displacement volume, but also to maintain a reasonable cooling size. The present study wishes to address this requirement and establish a relationship for the critical displacement volume requirements for future system design. Figure 8 shows a schematic of the cooling loop.

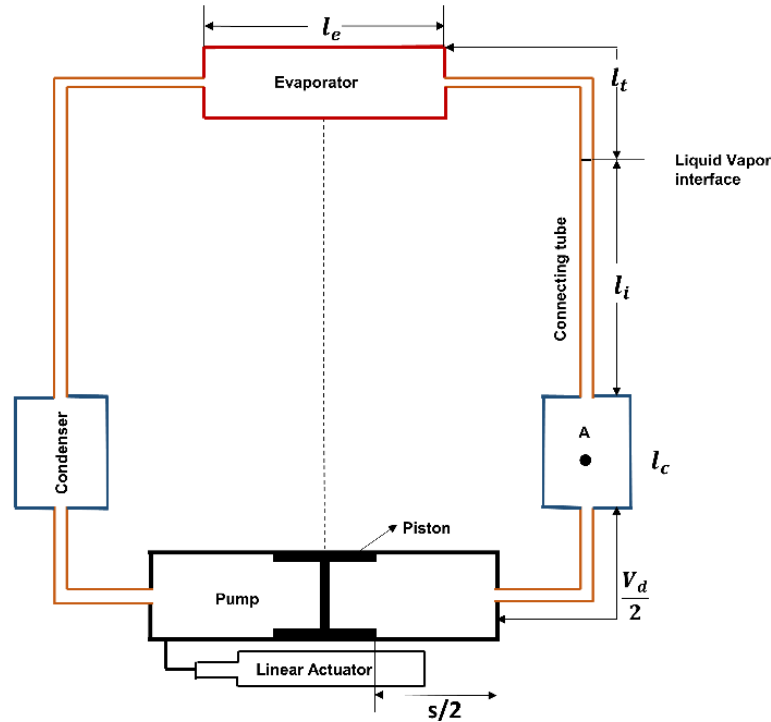


Figure 8. A schematic diagram of reciprocating-mechanism driven heat loop (RMDHL).

Due to the system nature, the cooling loop maintains condenser sections on both sides of the reciprocating driver and evaporator section. Hence, the cooling system can be considered as symmetric, with respect to the middle line between the reservoir and evaporator section. Therefore, the analysis of half of the loop is adequate enough to derive the critical displacement volume requirement. Regarding the right half of the loop, different section lengths and areas are termed via l and a , respectively, with their associated section's subscriptions (Condenser (c), evaporator (e), connecting tube (t)). Likewise, $V_d/2$ indicates total interior volume from the piston right dead end to the condenser section, a_p represents the piston cross-sectional area, and s is defined as the stroke of the reciprocating driver. In the course of the operation, the vapor produced in the evaporator section moves the liquid in the direction of the condenser section with a liquid–vapor interface (Figure 8). The thin liquid layers may have been generated on the evaporator's internal surface. However, it is ignored in the present analysis. Thus, the critical working condition is thought to be achieved when the condenser's center liquid, designated by A, can just reach or cross the evaporator midsection during piston movement, from the middle to right dead center. Mathematically, it can be written as follows:

$$a_p \frac{s}{2} + \frac{V_d}{2} + a_c l_c + a_t l_t \geq \frac{V_d}{2} + a_c l_c + a_t l_t + \frac{1}{2} a_e l_e + \frac{1}{2} a_c l_c + a_t l_t \tag{5}$$

Simplifying Equation (5), we have:

$$a_p s \geq a_c l_c + 2a_t l_t + a_e l_e \tag{6}$$

The above equation can be rewritten as:

$$a_p s \geq 2\left(\frac{1}{2} a_c l_c + a_t l_t + \frac{1}{2} a_e l_e\right) \tag{7}$$

The right-hand side of Equation (7) represents the total interior volume between the condenser center and evaporator center. It is considered as an important geometric parameter for its successful deployment. If the total interior volume is termed as effective displacement volume, afterward:

$$V_{eff} = 2\left(\frac{1}{2}a_c l_c + a_t l_t + \frac{1}{2}a_e l_e\right) \tag{8}$$

Equation (7) can be expressed as follows:

$$a_p s \geq V_{eff} \tag{9}$$

To achieve the system maximum potential, Equation (9) specifies that, $a_p s$ must be equal to or greater than V_{eff} . It specifies that the piston’s liquid displacement volume must be equal to or larger than the cooling loop’s effective displacement volume. For our present experiment, the minimum stroke used is about 2 cm, and cross-section of the pipe is uniform:

$$\begin{aligned} V_{eff} &= 2\left(\frac{1}{2}a_c l_c + a_t l_t + \frac{1}{2}a_e l_e\right) = 2 \times a_c(0.5 \times l_c + l_t + 0.5 \times l_e) \\ &= 2 \times \frac{\pi}{4}0.007^2(0.5 \times 0.24 + 0.14 + 0.5 \times 0.139) = 2.54 \times 10^{-5} \text{ m}^3 \\ a_p s &= \frac{\pi}{4}0.11^2 \times 0.02 = 1.9 \times 10^{-4} \text{ m}^3 \end{aligned}$$

Therefore, the present experiment satisfies Equation (9).

The derived relation for the critical displacement volume, Equation (9), is also employed for three prior successful loop designs on RMDHL, and the outcomes are presented in Table 1, including the result of the present study. Since all four designed loops worked properly and satisfied Equation (9), thus, Equation (9) can be used as a design criterium of RMDHLs. It should be noted that the referenced studies in Table 1 are all prior studies on RMDHLs.

Table 1. Critical displacement volume requirements.

	Liquid Displacement Volume, $a_p s$ (m ³)	Effective Displacement Volume, V_{eff} (m ³)	$a_p s \geq V_{eff}$
Present Study	2.54×10^{-5}	1.9×10^{-4}	Satisfied
Cao and Gao [22]	1.14×10^{-5}	9.9384×10^{-6}	Satisfied
Popoola [21]	3.6×10^{-4}	2.537×10^{-6}	Satisfied
Cao et al. [27]	2.85×10^{-4}	2.24×10^{-4}	Satisfied

5. Conclusions

The study aim was to analyze the performance, as well as the effect, of different important parameters on the performance of a reciprocating cooling loop. A bellows-driven reciprocating device was developed to study the effects of the amplitude, frequency of the reciprocating flow, surface heat flux, and the inlet temperature of the cooling water on the temperature distribution on the surface of a heated tube. The results showed that, as the amplitude of the reciprocating flow increased, the surface temperature decreased in the cooling loop. However, a moderate reciprocating frequency would produce the best data, in terms of lower temperature levels with minimized temperature gradients. Moreover, the effect of the inlet temperature on the surface temperature of the heated tube is not significant compared to the other parameters. To provide a broader use of the data, a correlation in terms of dimensionless effective conductance was developed. In addition, an analytical relation has been derived, which clearly illustrates the critical working fluid displacement volume requirement that should be considered during system design. The derived relation is employed for four design cases, with satisfactory outcomes.

Author Contributions: Conceptualization, M.D.A.; data curation, M.D.A. and M.A.; formal analysis, M.A., M.D.A. and S.S.; investigation, M.D.A.; methodology, M.D.A. and S.S.; resources, M.A.; supervision, Y.C.; writing—original draft preparation, M.D.A.; writing—review and editing, Y.C. All authors have read and agreed to the published version of the manuscript.

Funding: This research received no external funding.

Conflicts of Interest: The authors declare no conflict of interest.

Nomenclature

T	Temperature (K)
W	Watt ($\text{kg}\cdot\text{m}^2/\text{s}^3$)
k_{eff}	Effective thermal conductivity (W/mk)
k	Thermal conductivity (W/mk)
a	Area (m^2)
l	Length (m)
s	Reciprocating stroke (m)
V	Volume
U	Overall heat transfer ($\text{W}/\text{m}^2\text{ }^\circ\text{C}$)
h	Heat transfer coefficient ($\text{w}/\text{m}^2\cdot\text{K}$)
R	Thermal resistance ($\text{K}\cdot\text{m}/\text{w}$)
X	Amplitude (cm)
A_0	Dimensionless Amplitude
Re_ω	kinematic Reynolds number
D	Inner diameter (m)
W_0	Womersley number
P	Power (W)
F	Frequency
ρ	Density (kg/m^3)
\dot{m}	Mass flow rate (kg/s)
μ	Viscosity ($\text{N}\cdot\text{s}/\text{m}^2$)
p	Pressure (Pa)
ω	Reciprocating frequency (rad/s)
F	Force

Subscripts or Superscripts

t	tubing
c	condenser
e	evaporator
p	piston
eff	effective
w	wall

Appendix A

Different components of the experimental setup:



Polystat thermal bath
($-20\text{ }^\circ\text{C}$ to $150\text{ }^\circ\text{C}$)



P4400 Wattmeter (max power 1800
W)



Staco Power regulator
(0–120) V

Figure A1. Cont.



Figure A1. Different equipment in the test rig.

References

- Faghri, A. Heat pipes: Review, opportunities and challenges. *Front. Heat Pipes* **2014**, *1*, 5. [CrossRef]
- Fedorov, A.G.; Viskanta, R. Three-dimensional conjugate heat transfer in the microchannel heat sink for electronic packaging. *Int. J. Heat Mass Transf.* **2000**, *43*, 399–415. [CrossRef]
- Ganvir, R.B.; Walke, P.V.; Kriplani, V.M. Heat transfer characteristics in nanofluid—A review. *Renew. Sustain. Energy Rev.* **2017**, *75*, 451–460. [CrossRef]
- Kamdern, K.; Aurélien, C.; Zhu, X. Numerical Study on the Flow and Heat Transfer Coupled in a Rectangular Mini-Channel by Finite Element Method for Industrial Micro-Cooling Technologies. *Fluids* **2020**, *3*, 151. [CrossRef]
- Al-Rifai, S.; Lin, C.-X. Heat and Mass Transfer Correlations for Staggered Nanoporous Membrane Tubes in Flue Gas Crossflow. *J. Heat Transf.* **2022**, *144*, 062702. [CrossRef]
- Chen, C.; Hou, F.; Ma, R.; Su, M.; Li, J.; Cao, L. Design, integration and performance analysis of a lid-integral microchannel cooling module for high-power chip. *Appl. Therm. Eng.* **2021**, *198*, 117457. [CrossRef]
- Saha, S.; Khan, J.; Farouk, T. Numerical Study of Evaporation Assisted Hybrid Cooling for Thermal Powerplant Application. *Appl. Therm. Eng.* **2020**, *166*, 114677. [CrossRef]
- Gennaro, C.; Markussen, W.B.; Meyer, K.E.; Palm, B.; Kærn, M.R. Experimental characterization of the heat transfer in multi-microchannel heat sinks for two-phase cooling of power electronics. *Fluids* **2021**, *2*, 55.
- Marine, N.; Lips, S.; Sartre, V. Experimental investigation of a confined flat two-phase thermosyphon for electronics cooling. *Exp. Therm. Fluid Sci.* **2018**, *96*, 516–529.
- Poachaiyapoom, A.; Leardkun, R.; Mounkong, J.; Wongwiset, S. Miniature vapor compression refrigeration system for electronics cooling. *Case Stud. Therm. Eng.* **2018**, *13*, 100365. [CrossRef]
- Sohel Murshed, S.M.; Nieto De Castro, C.A. A critical review of traditional and emerging techniques and fluids for electronics cooling. *Renew. Sustain. Energy Rev.* **2017**, *78*, 821–833. [CrossRef]
- Mackley, M.; Stonestreet, P. Heat transfer and associated energy dissipation for oscillatory flow in baffled tubes. *Chem. Eng. Sci.* **1995**, *50*, 2211–2224. [CrossRef]
- Bouvier, P.; Stouffs, P.; Bardon, J.-P. Experimental study of heat transfer in oscillating flow. *Int. J. Heat Mass Transf.* **2005**, *48*, 2473–2482. [CrossRef]
- Zhao, T.; Cheng, P. Experimental studies on the onset of turbulence and frictional losses in an oscillatory turbulent pipe flow. *Int. J. Heat Fluid Flow* **1996**, *17*, 356–362. [CrossRef]
- Pandey, L.; Singh, S. Numerical Analysis for Heat Transfer Augmentation in a Circular Tube Heat Exchanger Using a Triangular Perforated Y-Shaped Insert. *Fluids* **2021**, *6*, 247. [CrossRef]
- Aligoodarz, M.R.; Mehrpanahi, A.; Moshtaghzadeh, M.; Hashiehbaf, A. Improved Criteria for Stall-Free Preliminary Design of Axial Compressor of Aero Gas Turbine Engines. *Proc. Inst. Mech. Eng. Part G J. Aerosp. Eng.* **2019**, *233*, 3286–3297. [CrossRef]
- McEvoy, J.; Sajad, A.; Tim, P. Experimental investigation of flow pulsation waveforms in rectangular mesochannels for high heat flux electronics cooling. *Exp. Therm. Fluid Sci.* **2019**, *109*, 109885. [CrossRef]
- Cao, Y.; Alam, M.D.; Popoola, O.T. Mechanically driven oscillating flow cooling loops—A review. *Front. Heat Mass Transf.* **2019**, *13*, 17. [CrossRef]
- Cao, Y.; Gao, M. Reciprocating-Mechanism Driven Heat Loop. U.S. Patent 6,684,941, 3 February 2004.
- Popoola, O.T.; Cao, Y. Investigation of a reciprocating driven heat loop to high heat single phase liquid cooling for temperature uniformity. *Glob. J. Res. Eng.* **2017**, *17*. Available online: <https://engineeringresearch.org/index.php/GJRE/article/view/1620> (accessed on 5 April 2022).
- Popoola, O.T. Numerical, Analytical, and Experimental Studies of Reciprocating-Mechanism Driven Heat Loops for High Heat Flux Cooling. Ph.D. Thesis, FIU, Miami, FL, USA, 2017.
- Cao, Y.; Gao, M. Experimental and Analytical Studies of Reciprocating-Mechanism Driven Heat Loops (RMDHLs). *J. Heat Transf.* **2008**, *130*, 072901. [CrossRef]
- Soleimanikutanaei, S.; Almas, M.; Popoola, O.T.; Cao, Y. Reciprocating liquid-assisted system for electronic cooling applications. *Heat Transf. Asian Res.* **2018**, *48*, 286–299. [CrossRef]
- Popoola, O.; Bamgbade, A.; Cao, Y. A Numerical Model of a Reciprocating-Mechanism Driven Heat Loop for Two-Phase High Heat Flux Cooling. *J. Therm. Sci. Eng. Appl.* **2016**, *8*, 041006. [CrossRef]

25. Popoola, O.; Cao, Y. The influence of turbulence models on the accuracy of CFD analysis of a Reciprocating-Mechanism driven heat loop. *Case Stud. Therm. Eng.* **2016**, *8*, 277–290. [[CrossRef](#)]
26. Sert, C.; Beskok, A. Numerical Simulation of Reciprocating Flow Forced Convection in Two-Dimensional Channels. *J. Heat Transf.* **2003**, *125*, 403–412. [[CrossRef](#)]
27. Cao, Y.; Xu, D.; Gao, M. Experimental study of a bellows-type reciprocating-mechanism driven heat loop. *Int. J. Energy Res.* **2012**, *37*, 665–672. [[CrossRef](#)]
28. Rahman, S.M.M.; Karim, K.E. Investigation of Heat Transfer Characteristics of a Water to Water Heat Exchanger: An Experimental Approach. In Proceedings of the International Conference on Mechanical Engineering and Renewable Energy 2015, Chittagong, Bangladesh, 26–29 November 2015.
29. Alam, M.D.; Hossain, S.T.; Simanto, H.S.; Shoyeb, M.; Mithu, U. Experimental and Numerical Investigation of an Air to Water Heat Exchanger. In Proceedings of the 3rd International Conference on Mechanical, Industrial and Energy Engineering 2014, Khulna, Bangladesh, 26–27 December 2014.
30. Cooper, W.L.; Nee, V.W.; Yang, K.T. An experimental investigation of convective heat transfer from the heated floor of a rectangular duct to a low frequency, large tidal displacement oscillatory flow. *Int. J. Heat Mass Transf.* **1994**, *37*, 581–592. [[CrossRef](#)]